The Astrophysical Journal, 824:15 (7pp), 2016 June 10 doi:10.3847/0004-637X/824/1/15

ORBITAL CIRCULARIZATION OF HOT AND COOL *KEPLER* ECLIPSING BINARIES

Vincent Van Eylen[1,2], Joshua N. Winn[2,3], and Simon Albrecht[1]
[1] Stellar Astrophysics Centre, Department of Physics and Astronomy, Aarhus University, Ny Munkegade 120, DK-8000 Aarhus C, Denmark; vincent@phys.au.dk
[2] MIT Kavli Institute for Astrophysics and Space Research, 70 Vassar Street, Cambridge, MA 02139, USA
[3] MIT Physics Department, 77 Mass. Avenue Cambridge, MA 02139, USA
Received 2015 September 10; accepted 2016 March 23; published 2016 June 3

ABSTRACT

The rate of tidal circularization is predicted to be faster for relatively cool stars with convective outer layers, compared to hotter stars with radiative outer layers. Observing this effect is challenging because it requires large and well-characterized samples that include both hot and cool stars. Here we seek evidence of the predicted dependence of circularization upon stellar type, using a sample of 945 eclipsing binaries observed by *Kepler*. This sample complements earlier studies of this effect, which employed smaller samples of better-characterized stars. For each *Kepler* binary we measure $e\cos\omega$ based on the relative timing of the primary and secondary eclipses. We examine the distribution of $e\cos\omega$ as a function of period for binaries composed of hot stars, cool stars, and mixtures of the two types. At the shortest periods, hot–hot binaries are most likely to be eccentric; for periods shorter than four days, significant eccentricities occur frequently for hot–hot binaries, but not for hot–cool or cool–cool binaries. This is in qualitative agreement with theoretical expectations based on the slower dissipation rates of hot stars. However, the interpretation of our results is complicated by the largely unknown ages and evolutionary states of the stars in our sample.

Key words: binaries: eclipsing – planets and satellites: dynamical evolution and stability – stars: evolution – stars: fundamental parameters

Supporting material: machine-readable table

1. INTRODUCTION

Binary stars make up over half of all stars in the universe, and their orbital properties have been studied for many decades (see, e.g., Kopal 1956). In close binary systems, tidal forces distort the shapes of stars and cause oscillations. The gradual dissipation of energy associated with those fluid motions ultimately leads to coplanarization and synchronization of rotational and orbital motion, as well as circularization of the binary orbit (see, e.g., Mazeh 2008, and references therein).

One interesting aspect of tidal circularization theory is that the dissipation rate is a very strong function of the orbital semimajor axis, and thereby on the orbital period (see, e.g., Zahn 1975). Many efforts have been made to determine the so-called "cutoff period" (see, e.g., Mayor & Mermilliod 1984), which characterizes the transition between mainly circular and mainly eccentric orbits. It has also been suggested that the cutoff period can serve as a proxy for age in star clusters (Mathieu & Mazeh 1988), and indeed there is evidence for a linear trend between the cutoff period and the age of binary stars in different clusters (e.g., Meibom & Mathieu 2005).

Another interesting aspect of the theory is that the circularization timescale is predicted to depend strongly on stellar type. Stars with thick exterior convective zones are expected to experience more rapid tidal dissipation than stars with mainly radiative exteriors (Zahn 1975). Our interest in this topic was heightened by some recent developments in exoplanetary science. The obliquities of the host stars of close-in giant planets have been observed to have different distributions for hot and cool stars (Winn et al. 2010; Albrecht et al. 2012), with the boundary between these types of stars at around $T_{\rm eff} \approx 6250$ K. It has been proposed that the differences in the obliquity distributions of cool and hot stars are due to differences in tidal dissipation, and perhaps magnetic braking (Dawson 2014).

Investigating these possibilities led us to search the literature for clear observational evidence of the dependence of tidal dissipation rates on effective temperature. The literature does provide some evidence for the expected dependence of the cutoff period on stellar type, mainly through the comparison of different samples that have been analyzed in different ways. This is at least partly because cool stars and hot stars have been studied by different communities using different techniques. For hot stars, Giuricin et al. (1984) found circularization below a period of 2 days for a sample of about 200 binary stars, which is seemingly consistent with the tidal friction theory of Zahn (1977). A similar result was arrived at more recently by Khaliullin & Khaliullina (2010), who compiled a catalog of about 100 eclipsing binaries from different sources. For cool stars, Koch & Hrivnak (1981) investigated binaries with periods shorter than 20 days, and found reasonable agreement with theory. Abt (2006) collected eccentricities for cool stars and found cutoff periods at around 4 days. Pourbaix et al. (2004) maintain a large catalog of eclipsing binaries that includes both hot and cool stars, but the catalog is an inhomogeneous concatenation of various sources, and does not lend itself to statistical studies. The most convincing study to date was performed by Torres et al. (2010), who studied 95 eclipsing binaries with masses and radii known to better than 3%. They found that short-period binaries tend to have circular orbits; long-period binaries have a wider range of eccentricities; and the critical period separating these regimes is larger for binaries with cool stars (defined by those authors as stars with $T_{\rm eff} < 7000$ K) than for binaries with hot stars.

Exoplanetary science has now provided an opportunity to perform a complementary study using a larger sample of less well-characterized binaries. The NASA *Kepler* mission (Borucki et al. 2010) was designed to find transiting planets, and also discovered thousands of eclipsing binaries (Prša

et al. 2011; Slawson et al. 2011). The *Kepler* photometry can be used to precisely determine one component of orbital eccentricity: $e\cos\omega$, the product of the eccentricity and the cosine of the argument of pericenter, which is related to the relative timing of the primary and secondary eclipses. The measured eclipse durations can also be used to determine $e\sin\omega$, though this is less straightforward. These photometric constraints on eccentricity are much easier to obtain than the task of measuring the orbital eccentricity through radial-velocity monitoring (see, e.g., Mazeh et al. 2006). Although Slawson et al. (2011) modeled a large number of *Kepler* EBs, the results for eccentricity were not reliable, presumably because their neural-network approach was designed to measure many different properties for a wide variety of binary stars and was not trained specifically to determine eccentricities.

Here, we employ a simpler method to measure $e\cos\omega$ reliably, based only on the relative timing of the primary and secondary eclipses. We combine these measurements with published effective temperatures for the binary components (Armstrong et al. 2014) to divide our sample into hot–hot, hot–cool, and cool–cool binaries. We then compare the observed $e\cos\omega$—period diagrams for these different categories of EBs. Thus, our study benefits from a relatively large sample and from homogeneity in the measurement techniques. However, it has the significant drawback that the masses, sizes, ages, and evolutionary states of the stars are not nearly as well-known as the systems studied by Torres et al. (2010).

This paper is organized as follows. Section 2 describes our sample and measurement techniques. Section 3 presents the results. Section 4 compares our results to simple theoretical expectations of tidal dissipation rates, taking into account systematic differences in stellar age. Finally, a discussion is presented in Section 5.

2. METHODS

2.1. Measuring $e\cos\omega$

To create our sample we begin with the EB catalog by Slawson et al. (2011).[4] We use the periods given in this catalog. We rely on the effective temperatures for the primary and secondary stars, T_1 and T_2, which were determined by Armstrong et al. (2014) by fitting the observed spectral energy distribution. We impose the restriction $T_{\rm eff}\leqslant 10{,}000$ K, to limit the number of very young stars in the sample and thereby simplify the interpretation, as described in more detail in Section 4. To measure $e\cos\omega$, we determine the times of primary and secondary eclipses using the procedure described below.

The *Kepler* observations are separated into different quarters (Q), each representing about three months of data. The data from each quarter are provided in three separate files, each containing one month of data. Our starting point is the pre-search data conditioning (PDC) photometry, from which some of the instrumental trends have been removed (Smith et al. 2012). For normalization, we divide the flux data from each month by the mean monthly flux level. The data are then folded based on the period reported in the Villanova EB catalog (Slawson et al. 2011), and binned in orbital phase by a factor of 50.

[4] We use an updated version that is available online at http://keplerebs.villanova.edu/, accessed on 2015 March 9.

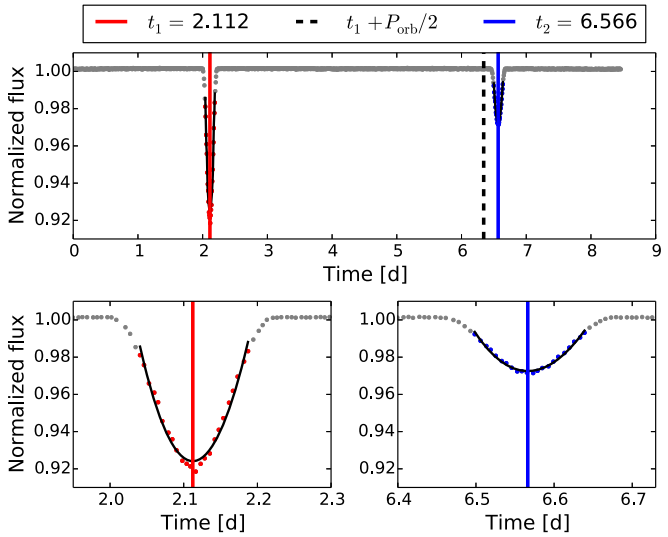

Figure 1. Sample output from our code for finding primary and secondary eclipse times. The colored data points are fitted to determine the eclipse times; the results are marked by thick vertical lines. The dotted vertical line indicates the expected location of the secondary eclipse, for a circular orbit. The bottom panels allow a closer inspection of the narrow time ranges surrounding the primary and secondary eclipses.

Subsequently we determine the times of the primary and secondary eclipses. We do so as follows: first, we locate the approximate time of the deepest eclipse (t_1). The time interval containing this eclipse is then ignored, and we determine the approximate time of the second eclipse (t_2). We determine the precise times by fitting a second-order polynomial function of time to the data near minimum light. We estimate uncertainties by using a bootstrap technique. We create 100 samples by drawing randomly (with repetitions allowed) from the actual data points. We then refit these samples, and adopt the mean of the results as the "best value," and the standard deviation of the results as the 1σ uncertainty.

We then find $e\cos\omega$, using

$$e\cos\omega \approx \frac{\pi\,(t_2 - t_1)}{2P} - \pi/4, \qquad (1)$$

where P is the orbital period.[5] The method is illustrated in Figure 1.

We apply this method to all stars in the EB catalog (Slawson et al. 2011) that have orbital periods between 1.5–50 days. Binary systems with periods shorter than 1.5 days are often non-detached, which complicates the measurements. These binaries are not likely to be useful for our study because they have been found to be circularized regardless of stellar type (Torres et al. 2010). Likewise, for binaries with periods longer than 50 days, tidal circularization is very likely irrelevant for all types of binaries.

In some cases, our automated method fails to identify the correct eclipse times due to data artifacts. These systems are manually refitted. To avoid any bias, we perform this refitting blindly, i.e., the fitter has no knowledge of the stellar effective temperatures. In other cases there are no secondary eclipses, or no primary eclipses. We remove these cases from consideration, after confirming the absence of the eclipses through visual

[5] Note that this equation is only approximate and correction factors apply for high eccentricity; see, e.g., Sterne (1940).

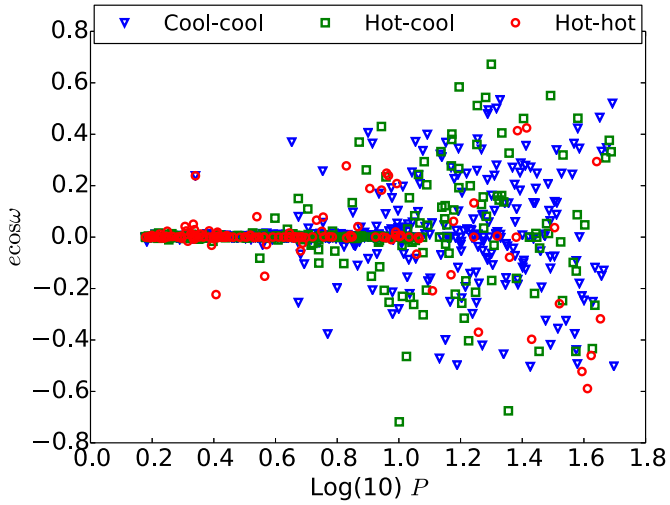

Figure 2. Measurements of $e\cos\omega$ as a function of orbital period. The red circles represent "hot–hot" binaries in which both stars have $T_{\rm eff} > 6250$ K. Blue triangles are for "cool–cool" binaries, and green squares are for binaries with one hot star and one cool star.

inspection of all the folded light curves. We do not think that these omissions produce any significant bias relating to stellar effective temperature, although we caution that highly eccentric binaries are more likely to only show either primary or secondary eclipses, which means that our derived distribution of $e\cos\omega$ (for all stellar temperatures) may be biased toward lower values.

3. RESULTS

The main result of our analysis is measurements of $e\cos\omega$ that are associated with the previously determined orbital period P (from Slawson et al. 2011) and the stellar temperatures of the two components (from Armstrong et al. 2014). Figure 2 shows the measurements of $e\cos\omega$ as a function of P, with the color of each circle encoding the effective temperatures of the components. Following Winn et al. (2010) and Albrecht et al. (2012), we use 6250 K as the boundary between "hot" and "cool" stars. A binary is designated "hot–hot" if both stars have estimated effective temperatures exceeding this nominal boundary value. Likewise, "cool–cool" binaries have two cooler stars, and "hot–cool" binaries have one hot star and one cool star. We present results for 137 hot–hot binaries, 289 hot–cool binaries, and 519 cool–cool binaries. The parameters for all EBs in our sample are reported in Table 1.

Figure 2 shows that the distribution of $e\cos\omega$ is roughly symmetric around zero, as would be expected for a uniform random distribution of ω, the argument of pericenter. At the shortest periods, it is clear that most binaries are circular or nearly circular. The spread in eccentricity increases with increasing orbital period. This is consistent with what is expected from tidal circularization at short periods, and with previous studies of other samples.

Figure 3 shows the fraction of EBs that are significantly eccentric, within different period bins. In this analysis, we use $|e\cos\omega| \geqslant 0.02$ as our criterion for significant eccentricity. The error bars displayed on the bins represent only the uncertainty due to Poisson (counting) statistics. It is clear that beyond 10–15 days, the large majority of binaries are eccentric regardless of the temperature. At shorter periods, this is not the case. The fraction of eccentric binaries decreases with decreasing period, and it does so at different rates for different temperature classes. For $P \leqslant 10$ days, the hot–hot binaries have a greater fraction of eccentric systems at a given period.

4. COMPARISON WITH THEORY

The observed eccentricity of an EB depends on its initial eccentricity, the rate of tidal circularization, and the time interval over which circularization has taken place, i.e., the age of the system. For simplicity we assume that the initial eccentricity distribution is broad and is the same for binaries of all types (although we are not aware of any firm observational support for this latter assumption). Thus, in our model, any differences in eccentricity distributions between samples of EBs come from differences in tidal dissipation rates and ages.

To calculate the expected timescales for tidal circularization for convective stars ($\tau_{\rm conv}$) and for radiative stars ($\tau_{\rm rad}$), we follow Claret & Cunha (1997) and use the formulas

$$\tau_{\rm circ,conv} = (1.99 \times 10^3\ {\rm yr}) M^3 \frac{(1+q)^{5/3}}{q} L^{-1/3} \lambda_2^{-1} \frac{P^{16/3}}{R^{22/3}} \quad (2)$$

and

$$\tau_{\rm circ,rad} = (1.71 \times 10^1\ {\rm yr}) M^3 \frac{(1+q)^{5/3}}{q} E_2^{-1} \frac{P^7}{R^9}, \quad (3)$$

where M and R are the total stellar mass and radius in solar units, q is the mass ratio of the two stars, and L is the total luminosity relative to the Sun's luminosity. For simplicity we assume the main-sequence relations $L \propto M^{3.9}$ and $R \propto M^{0.8}$, and we set $q = 1$. We use representative values for E_2 and λ_2 (Claret & Cunha 1997, see their Figures 1 and 3). We can now calculate the circularization timescale for convective and radiative stars of different masses and periods.

As for the age, our estimate is based on the simple and approximate main-sequence relationship, $\tau_\star = (10^{10}\,{\rm yr})(M/M_\odot)^{-2.9}$. While ages of individual *Kepler* EBs are typically unknown, on average the hot stars are expected to be systematically more massive, faster-evolving, and younger, giving them less time for tidal dissipation to circularize their orbits.

We can now calculate the relative circularization time $\tau_{\rm circ}/\tau_\star$ as a function of period for different systems. Figure 4 shows some illustrative results. For values of $\tau_{\rm circ}/\tau_\star$ that greatly exceed unity, we expect to observe a broad distribution of eccentricities because the lifetime of the system is too short to have allowed for significant circularization. For values of $\tau_{\rm circ}/\tau_\star$ that are well below unity, the opposite is true, and we expect most binaries to have circular orbits.

According to the results of this rough calculation, we should expect to find a critical circularization period for cool stars in the neighborhood of 5 days ($\log P = 0.7$). For hot stars we should find a shorter circularization period depending more strongly on mass, ranging from about 1.3 days for $10\,M_\odot$ to 3 days for $2\,M_\odot$. We emphasize that these exact numbers depend on a range of assumptions outlined above, and should be considered as rough estimates rather than exact predictions.

To isolate the theoretical effect of tidal dissipation, as opposed to stellar age, Figure 4 shows the results after setting $\tau_\star$ equal to the Hubble time for all cases. Here there are no relative age effects at play. By comparing the two panels in this figure we see that the effect of age is important for the most massive stars (which are on average the youngest). For the hot

Table 1
System Parameters for *Kepler* Eclipsing Binaries with Measured $e \cos \omega$ Values

KIC	Period (d)	Ephemeris (HJD)	T_1 (K)	σ (T_1) (K)	T_2 (K)	σ (T_2) (K)	$e \cos \omega$	σ ($e \cos \omega$)
1026032	8.46044	54966.77381	6149	359	4863	556	0.0416	0.0005
1433980	1.59263	55000.37409	6869	370	5484	558	−0.0014	0.0021
1571511	14.02245	54954.50475	5946	363	6023	684	0.0465	0.0021
1575690	2.25243	54965.43526	4207	370	3776	570	−0.0015	0.0008
1725193	5.92769	55005.64981	6044	354	5988	554	0.0002	0.0008
2019076	7.12923	55004.07222	6199	360	5184	561	0.0	0.0008
2161623	2.28347	54999.59984	7045	765	5106	1085	0.0049	0.0048
2162994	4.10159	54965.63165	5823	357	5684	551	0.0003	0.0007
2167890	2.6483	55185.84325	4878	370	4765	623	0.008	0.0074
2306740	10.30699	54966.42521	6060	368	5769	656	0.0238	0.0006
2308957	2.21968	54965.16646	5993	363	5825	562	0.0016	0.001
2309587	1.83851	54965.10135	5765	381	5576	773	0.0019	0.0013
2437060	3.18711	55000.89072	4930	357	3860	576	0.0027	0.0096
2437149	18.79874	55008.62182	5456	361	5165	624	−0.0165	0.0022
2437452	14.46993	54974.81653	5488	360	4552	609	0.0012	0.0005
2437783	7.45341	55002.00678	6149	1599	6343	2474	0.0042	0.0041
2438061	4.88585	55004.09363	5278	356	4559	567	−0.0001	0.0009
2438490	3.31577	55001.02005	5459	376	5220	683	−0.009	0.0061
2441161	4.38398	55004.68452	5501	362	4887	570	−0.0016	0.0007
2442084	49.7886	55008.19209	3970	352	3819	553	−0.5019	0.0014

(This table is available in its entirety in machine-readable form.)

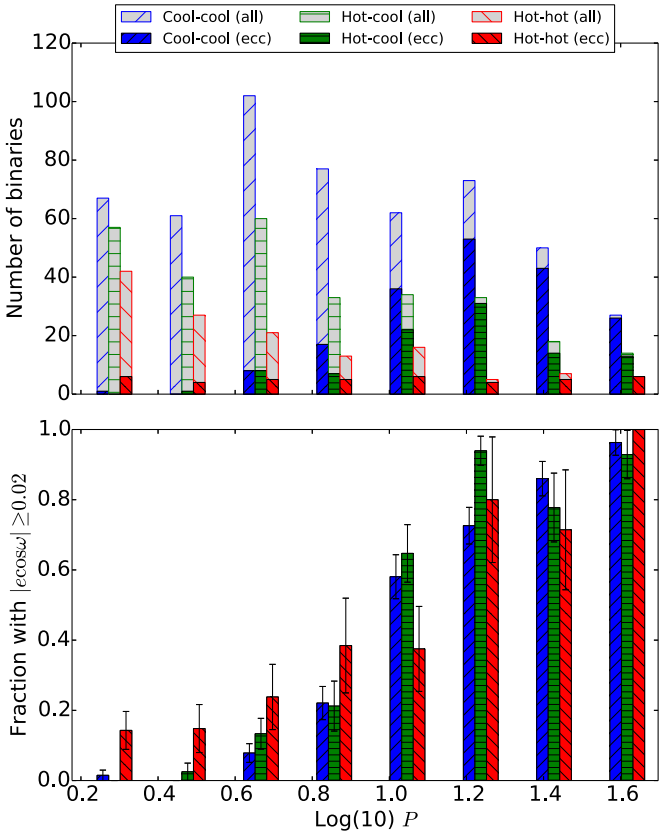

Figure 3. Top: histogram of the binaries in (logarithmic) period bins, divided into hot–hot, hot–cool, and cool–cool binaries. The eccentric binaries, defined as $|e \cos \omega| \geqslant 0.02$, are highlighted. Bottom: the fraction of eccentric binaries per bin.

stars, replacing the stellar age with the much longer Hubble time results in longer circularization periods. Thus, in this simple picture, stars with a mass of $5\,M_\odot$ have a similar tidal dissipation rate as cooler, lower-mass stars with thick convective zones, but we should nevertheless observe such stars to have a shorter circularization period because of their younger ages. For even more massive stars the age effect becomes even more dominant. For the case of $10\,M_\odot$, the circularization period actually *exceeds* that of the cooler stars. On the other hand, for stars of mass $2\,M_\odot$, age effects are much less important. This is understandable, since the typical lifetimes of such stars are only a few times shorter than those of subsolar mass stars.

These theoretical considerations show that for the purpose of observing the specific dependence of tidal dissipation rates on stellar type, it is important to focus on stars that are not too massive (too hot). We are thereby led to limit our sample to $M \leqslant 3\,M_\odot$. Since $T_{\rm eff}/T_{\rm eff,\odot} \approx \sqrt{M/M_\odot}$ on the main sequence, this is achieved by restricting $T_{\rm eff} \leqslant 10{,}000$ K.

Based on Figure 4 we expected that cool–cool binaries would mainly be circular below ≈5 days ($\log P = 0.7$), with the precise "cutoff" period almost independent of stellar mass. For hot–hot binaries we expected that for periods exceeding 2–3 days ($\log P = 0.3$–0.5), some systems could remain eccentric, with the precise cutoff period depending more strongly on stellar mass, leading to a greater scatter. For hot–cool systems, the cool component is expected to provide most of the tidal dissipation, leading us to expect the cutoff period for hot–cool systems to be similar to that for cool–cool systems.[6]

Qualitatively, these are indeed the trends that are observed. Figure 5 allows a closer inspection of the systems with periods shorter than five days. At the shortest periods, a clear difference is observed between stars with different temperatures. For example, at periods between 1.5 and 4 days, there are 74 hot–hot stars, of which 12 show significant eccentricity (which, as before, is defined as $|e \cos \omega| \geqslant 0.02$). By contrast, there are

[6] In reality the situation may be more complex if the hot component is significantly more massive because the total mass affects the orbital separation at a given orbital period. We have not attempted to correct for this effect given the coarse knowledge of stellar masses in our sample.

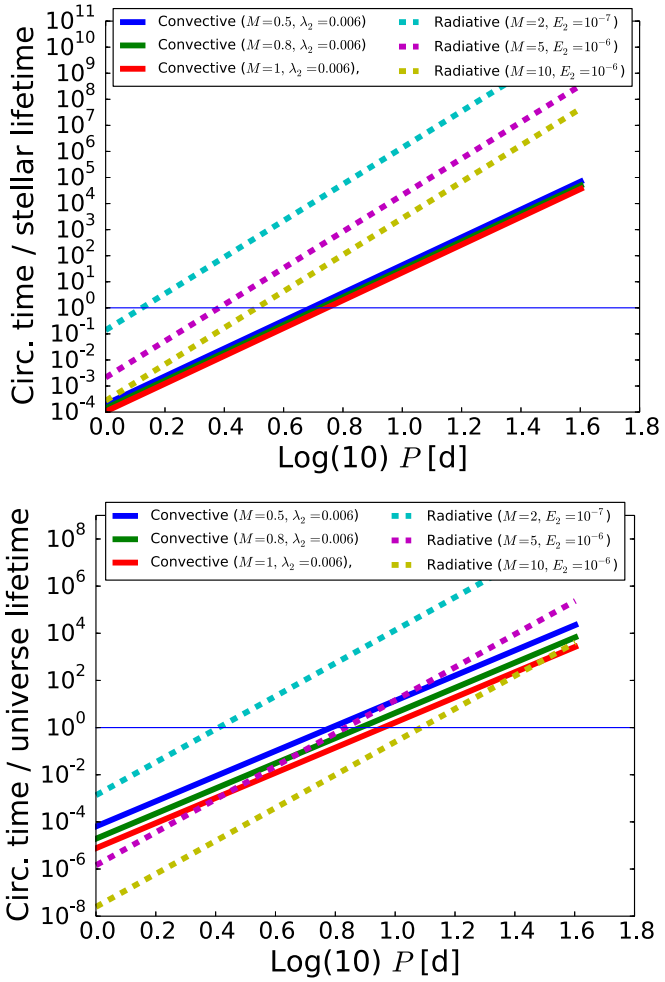

Figure 4. Top: the circularization timescales for convective (Equation (2)) and radiative (Equation (3)) stars, divided by the typical lifetime of such stars. Numbers above unity indicate that most of these systems have not had time to circularize, while numbers below unity indicate a circularization timescale shorter than the lifetime of the system. Bottom: rather than dividing by the stellar lifetime, we have now divided by the age of the universe. If the most massive stars lived this long, they would circularize up to longer periods than they do, but stars of a few solar masses are much less affected.

156 cool–cool and 108 hot–cool stars, and only 2 stars in each category have a significant eccentricity. For periods between 4 and 5 days, some eccentric systems occur for all stellar types: there are 2 out of 14 hot–hot systems showing eccentricity, 5 out of 54 for cool–cool systems, and 2 out of 29 for hot–cool systems.

In Figure 6, we show the cumulative fraction of systems with a significant eccentricity, $N_{\rm ecc}/N_{\rm all}(P)$. This is defined as

$$\frac{N_{\rm ecc}}{N_{\rm all}}(P) = \frac{N\,(P_\star \leqslant P \text{ and } |e\cos\omega| \geqslant 0.02)}{N\,(P_\star \leqslant P)}, \qquad (4)$$

where $N(P_\star \leqslant P)$ is the number of binary stars with periods less than or equal to P. From Figure 6, we see that hot–hot binaries show significant eccentricities at shorter periods than hot–cool or cool–cool binaries. The hot–cool and cool–cool binaries have a very similar period-dependence of their eccentricity distributions. At longer periods, the hot–cool and cool–cool binaries have a higher fraction of eccentric systems than the hot–hot binaries, presumably because the sample of hot–hot

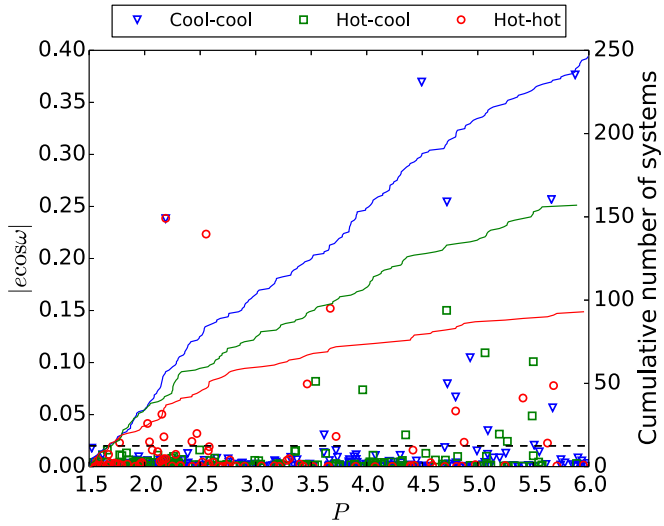

Figure 5. Measurements of $|e\cos\omega|$ as a function of orbital period in the period range of 2–6 days. The red circles represent "hot–hot" binaries in which both stars have $T_{\rm eff} > 6250$ K. Blue triangles are for "cool–cool" binaries, and green squares are for binaries with one hot star and one cool star. Despite the smaller number of hot–hot binaries, this category boasts the largest number of eccentric systems.

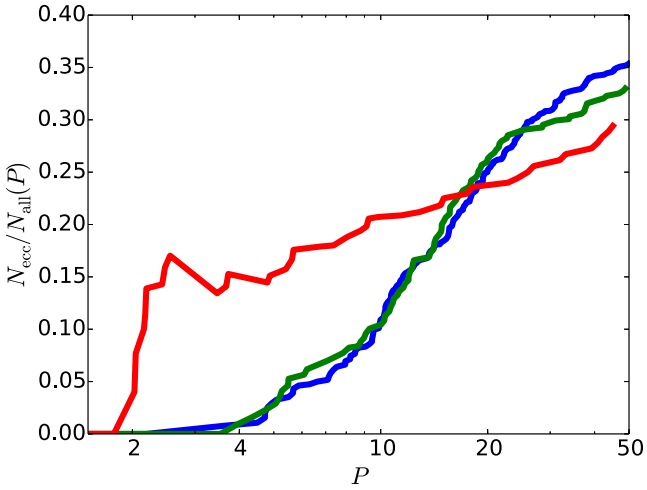

Figure 6. Cumulative fraction of eccentric systems, as defined in Equation (4). Hot–hot binaries can be eccentric at periods beyond about 2 days, while hot–cool and cool–cool binaries exhibit eccentricities at periods longer than 4–5 days.

binaries has a larger fraction of shorter-period systems (see Figure 3).

5. DISCUSSION

This work represents an attempt to compare the degree to which tidal circularization has taken place in binaries with hot and cool stars, using a large sample of *Kepler* eclipsing binaries that has been analyzed with homogeneous measurement techniques. The observations displayed in Figures 2 and 3 agree remarkably well with the predictions in Figure 4, despite the obvious limitations and simplicity of our crude theoretical calculations.

This suggests that we have indeed detected the dependence of orbital circularization on stellar type, due to the combination of age effects and differing tidal dissipation rates. The observations alone cannot tell us which of these two factors

—age or tidal dissipation—is more important. However, as pointed out in Section 4, for stars cooler than about 10,000 K, age effects are not expected to be dominant; the main effect should be tidal dissipation rates. Another suggestion that the differences in cutoff periods between the samples cannot be caused exclusively by differences in age is provided by the "mixed" binaries. In these cases one of the stars is hot and therefore evolving rapidly, causing these binary systems to be systematically younger than cool–cool binaries. Thus, in terms of age, the mixed binaries should be comparable to the hot–hot systems. However, we observe their eccentricity fraction at short periods to be lower than that of the hot–hot systems, which (in our admittedly simple framework) can only be explained by the higher tidal dissipation rate of the cool component in these systems.

Despite the advantages of a homogeneous analysis method and relatively large sample, there are also important limitations for our study. Rather than eccentricity itself, we chose to focus on $e\cos\omega$ because this parameter is so readily determined from the existing *Kepler* photometry. After some preliminary efforts, we abandoned the attempt to measure $e\sin\omega$, which can in principle be derived from the relative duration of the primary and secondary eclipses. We found that such measurements are considerably more complicated to make reliably, due to the covariance of this parameter with the semimajor axis, orbital inclination, and limb-darkening parameters. Even in favorable cases the precision in $e\sin\omega$ is typically an order of magnitude worse than in $e\cos\omega$. Nevertheless, it is likely that the measurements of both $e\cos\omega$ and $e\sin\omega$ can be improved upon for individual systems of interest. In addition, radial-velocity observations could be undertaken to validate these determinations.

In this work we have taken 6250 K to be the dividing line between hot stars with radiative outer layers and cool stars with convective outer layers. This choice was made for consistency with previous work on the obliquities of exoplanet host stars (Winn et al. 2010; Albrecht et al. 2012). However, other dividing lines have been used by other authors; for example, Torres et al. (2010) used 7000 K. If we use 7000 K as the dividing line, there are 8 hot–hot systems out of 34 with periods shorter than 4 days which exhibit a significant eccentricity (as opposed to 12 out of 74, for a dividing line of 6250 K). Furthermore, with the 7000 K boundary, there would be 6 out of 259 cool–cool eccentric systems, and 2 out of 45 hot–cool eccentric systems. This suggests that if we had chosen 7000 K, this would have strengthened the result that hot–hot binaries are more likely than hot–cool or cool–cool binaries to be eccentric at relatively short periods. We also note that Torres et al. (2010) did not impose an upper limit of 10,000 K, as we do here. A substantial fraction of the hot stars in their sample are substantially hotter than those considered here (the hottest stars in their sample are 38,000 K). As a result, the Torres et al. (2010) sample may be more affected by the systematic age differences between hot and cool stars.

We did not take into account the uncertainties in the stellar temperatures given by Armstrong et al. (2014). In some cases the uncertainties are substantial: the mean uncertainty for primary stars is 370 K. Undoubtedly some of the objects in our sample have been misclassified. This situation will improve after the EBs are studied spectroscopically. We also note that the calculations of T_2 relative to T_1 by Armstrong et al. (2014) may have a subtle dependence on eccentricity, because the $e\sin\omega$ parameter can affect the depth ratio between eclipses. We neglected this effect in this study.

There are also some issues to keep in mind regarding the theoretical interpretation. As pointed out in Section 4, we have assumed that the initial eccentricity distribution is the same for all stellar types, which is not necessarily the case. In addition, we do not generally know the age of individual binary stars. At this point we can only make general statements about systematic differences between our samples. In some cases the individual system ages could be derived from isochrone fitting, asteroseismology, or gyrochronology, although deriving ages for all EBs in the sample would require considerable effort. Furthermore, in our interpretation we have assumed that all stars in our sample are on the main sequence, using the scaling relations presented in Section 4. This is certainly not the case in reality, particularly for the hotter and faster-evolving stars. Furthermore, we assumed that all binaries with periods longer than 1.5 days are detached, but in reality some of them may be semi-detached.

We have attributed the differences in the eccentricity distribution, in part, to tidal effects, using simplified equations drawn from equilibrium and dynamical tidal circularization theory, as brought forward by Zahn (1975). In reality, the tidal circularization efficiency is probably itself a function of stellar evolution, i.e., it is not necessarily the same throughout the evolution of the system. We have furthermore neglected the possibility of additional stars in the systems, which may affect the eccentricity in individual cases (Mazeh & Shaham 1979). The probability of having third bodies is itself a (decreasing) function of orbital period (Tokovinin et al. 2006). It may be interesting to analyze the shortest-period binaries with non-zero eccentricities, to see if they can be explained by the presence of a third companion.

Despite this long list of limitations, we have shown in a relatively direct and homogeneous manner that the eccentricity distributions of hot–hot and cool–cool binaries are significantly different as a function of orbital period. This is likely caused by a combination of the different ages of the systems and a different tidal circularization efficiency. We anticipate that more detailed studies of (subsamples of) the *Kepler* EB sample will further constrain tidal circularization theory. We also expect our findings to be of interest in the context of tidal theory for stellar obliquities in double star systems (e.g., Albrecht et al. 2014) and in exoplanet systems (e.g., Winn et al. 2010; Albrecht et al. 2012).

We thank Kevin Schlaufman, Saul Rappaport, Jens Jessen-Hansen, and the anonymous referee for helpful comments and suggestions that have significantly improved this manuscript. Part of this manuscript was written at MIT and V.V.E. appreciates the hospitality of the researchers and staff at the MIT Kavli Institute for Astrophysics and Space Research. Work by J..N.W. was partly supported by funding from the NASA Origins program (grant ID NNX11AG85G). Funding for the Stellar Astrophysics Centre is provided by The Danish National Research Foundation (grant agreement No. DNRF106). The research is supported by the ASTERISK project (ASTERoseismic Investigations with SONG and *Kepler*) funded by the European Research Council (grant agreement No. 267864). We acknowledge ASK for covering travels in relation to this publication. Part of this work was

supported by the Danish Council for Independent Research, through a DFF Sapere Aude Starting grant No. 4181-00487B.

REFERENCES

Abt, H. A. 2006, ApJ, 651, 1151
Albrecht, S., Winn, J. N., Johnson, J. A., et al. 2012, ApJ, 757, 18
Albrecht, S., Winn, J. N., Torres, G., et al. 2014, ApJ, 785, 83
Armstrong, D. J., Gómez Maqueo Chew, Y., Faedi, F., & Pollacco, D. 2014, MNRAS, 437, 3473
Borucki, W. J., Koch, D., Basri, G., et al. 2010, Sci, 327, 977
Claret, A., & Cunha, N. C. S. 1997, A&A, 318, 187
Dawson, R. I. 2014, ApJL, 790, L31
Giuricin, G., Mardirossian, F., & Mezzetti, M. 1984, A&A, 134, 365
Khaliullin, K. F., & Khaliullina, A. I. 2010, MNRAS, 401, 257
Koch, R. H., & Hrivnak, B. J. 1981, AJ, 86, 438
Kopal, Z. 1956, AnAp, 19, 298
Mathieu, R. D., & Mazeh, T. 1988, ApJ, 326, 256
Mayor, M., & Mermilliod, J. C. 1984, in IAU Symp. 105, Observational Tests of the Stellar Evolution Theory, ed. A. Maeder, & A. Renzini (Dordrecht: Reidel) 411
Mazeh, T. 2008, in EAS Publications Ser. 29, Tidal Effects in Stars, Planets and Disks, ed. M.-J. Goupil, & J.-P. Zahn (Les Ulis: EDP Sciences), 1
Mazeh, T., & Shaham, J. 1979, A&A, 77, 145
Mazeh, T., Tamuz, O., & North, P. 2006, MNRAS, 367, 1531
Meibom, S., & Mathieu, R. D. 2005, ApJ, 620, 970
Pourbaix, D., Tokovinin, A. A., Batten, A. H., et al. 2004, A&A, 424, 727
Prša, A., Batalha, N., Slawson, R. W., et al. 2011, AJ, 141, 83
Slawson, R. W., Prša, A., Welsh, W. F., et al. 2011, AJ, 142, 160
Smith, J. C., Stumpe, M. C., Van Cleve, J. E., et al. 2012, PASP, 124, 1000
Sterne, T. E. 1940, PNAS, 26, 36
Tokovinin, A., Thomas, S., Sterzik, M., & Udry, S. 2006, A&A, 450, 681
Torres, G., Andersen, J., & Giménez, A. 2010, A&ARv, 18, 67
Winn, J. N., Fabrycky, D., Albrecht, S., & Johnson, J. A. 2010, ApJL, 718, L145
Zahn, J.-P. 1975, A&A, 41, 329
Zahn, J.-P. 1977, A&A, 57, 383